Phases of daylight and the stability of color perception in the near peripheral human retina

Athanasios Panorgias Faculty of Life Sciences, The University of Manchester, Manchester, UK

Janus J. Kulikowski Faculty of Life Sciences, The University of Manchester, Manchester, UK

Neil R. A. Parry Manchester Academic Health Science Centre, Faculty of Medical and Human Sciences, The University of Manchester, Manchester, UK, & Vision Science Centre, Manchester Royal Eye Hospital, Manchester, UK

Declan J. McKeefry Bradford School of Optometry and Vision Sciences, University of Bradford, Bradford, UK

Ian J. Murray Faculty of Life Sciences, The University of Manchester, Manchester, UK

Typical daylight extends from blue (morning sky) to orangey red (evening sky) and is represented mathematically as the Daylight Locus in color space. In this study, we investigate the impact of this daylight variation on human color vision. Thirty-eight color normal human observers performed an asymmetric color match in the near peripheral visual field. Unique hues were identified using a naming paradigm. The observers' performance for matching was almost perfectly coincident with the Daylight Locus but declined markedly in other regions. Interobserver variability reached a conspicuous minimum adjacent to the Daylight Locus and was maximal in the red and yellowish-green regions. In the naming task, unique blue and yellow were virtually coincident with the Daylight Locus. The results suggest that the mechanisms of color perception mediated by the phylogenetically older (blue–yellow) color pathway have been strongly influenced by the different phases of daylight.

Keywords: color vision, peripheral retina, daylight, color vision variability, evolution, unique hues

Citation: Panorgias, A., Kulikowski, J. J., Parry, N. R. A., McKeefry, D. J., & Murray, I. J. (2012). Phases of daylight and the stability of color perception in the near peripheral human retina. *Journal of Vision, 12*(3):1, 1–11, http://www.journalofvision.org/content/12/3/1, doi:10.1167/12.3.1.

Introduction

The sensation of color for broadband distributions of light is commonly divided into "warm," "neutral," or "cool" depending on whether the wavelength mix in a particular source is biased toward redness or blueness. Similarly, clear early morning skylight, with its predominance of short wavelengths, is described as cool, while evening skylight, dominated by longer wavelengths, is warm. In humans, the appreciation of these wavelength shifts relies on the quantal catch of three different types of cone photoreceptor (Jacobs & Deegan, 1999). Postreceptoral mechanisms provide exquisite sensitivity to small wavelength differences. Although color vision is regarded as a speciality of the central field, the ability to accurately perceive color is retained at eccentricities of around 10° in most observers. Between 10° and 20°, systematic shifts in the perceived appearance of color stimuli have been described (Moreland & Cruz, 1959; Parry, McKeefry, & Murray, 2006). The nature of these shifts reflects the organization of color processing in the retina and subsequent structures, in particular the visual cortex.

Characteristics of terrestrial illumination

There is a well-developed argument that the evolution of all visual sensory mechanisms must have been strongly influenced by the characteristics of terrestrial illumination (Shepard, 1992). The earth spins on its axis and around

doi: 10.1167/12.3.1 Received October 25, 2011; published March 1, 2012 ISSN 1534-7362

the sun, with the result that daily terrestrial illumination follows a distinctive pattern. Because of air molecules and other microscopic particles in the atmosphere, the sun's radiation is subject to Rayleigh scatter that affects only short wavelengths, resulting in the blue appearance of the sky (Smith, 2005). The residual radiation is composed only of middle and long wavelengths, the average of which is in the yellow region of color space. So, Rayleigh scattering provides a blue–yellow chromatic variation (Shepard, 1992). As the sun approaches the horizon, its radiation penetrates longer and denser columns of air. Although the proximity of the horizon is the same at sunrise and sunset, the temperature is higher at sunset. This results in a greater proportion of water molecules that are larger than air molecules. These scatter the long-wavelength component of the sunlight, giving the distinct orangey-red sunset sky. Hence, the elevation of the sun and the presence of water vapor in the atmosphere result in a red–green chromatic variation. Of course, over a 24-h cycle, there is also an overall change in intensity of illumination from the very bright midday to the darkest starlit night. This intensity change is said to have provided the need for the extremely wide range of luminances to which visual systems are capable of responding (Shepard, 1992).

The various stages of daylight can be readily expressed in a color space (a mathematical representation of all additive color mixtures). These are described as the Daylight Locus (Wyszecki & Stiles, 1982), which divides the color space into warm, cool, and neutral colors. The Daylight Locus tracks the range of perceived sky colors from early morning blue sky to a distinct orangey-red sunset and is numerically described in terms of correlated color temperature, with high color temperatures corresponding to a blue tinge and lower color temperatures to a reddish tinge. Inevitably, there are day-to-day variations in the pattern of sky colors, depending on geographical and meteorological conditions. However, under a clear sky, the chromaticity gamut of daylight corresponds to high color temperatures in the mornings and relatively low color temperatures in the evenings (Nayatani & Wyszecki, 1963).

Primate color vision

Color vision in catarrhines (Old World monkeys, apes, and humans) is described as trichromatic. It is based on three cone types, each having a broad action spectrum but with maximum sensitivity (λ_{max}) in either the short (S-), medium (M-), or long (L-) wavelength region of the visible spectrum (Jacobs & Nathans, 2009; Nathans, 1987). Despite this wavelength specificity, each cone type shows some response to light across much of the visible spectrum. Early-stage color processing in the retina is mediated by the comparison of signals from the different classes of cones, which are combined to form two distinct chromatic pathways. The first, S-(L + M), mechanism extracts blue–yellow information. The second compares signals from L- and M-cones and conveys red–green information. Signals from L- and M-cones are added to form the luminance (L + M) pathway that mediates the perception of lightness–darkness (Hering, 1964; Hurvich & Jameson, 1955). Consistent with their phylogeny, the neurons that form the two chromatic pathways are quite different; they are strictly segregated anatomically and their morphological and physiological differences are clear in the retina and the lateral geniculate nucleus (Dacey, 2000; Dacey & Lee, 1994). These three cone-opponent pathways are almost certainly closely linked with the three variations of terrestrial illumination described above.

Most mammals possess two cone types, one containing a short-wavelength pigment ($\lambda_{max} \sim 400$ nm) and a second middle- to long-wavelength pigment ($\lambda_{max} \sim 510$–570 nm; Jacobs, 2009). These two cone types give rise to a single S–L dimension of color vision (blue–yellow variation). This dichromatic color vision has been confirmed in both behavioral and histological studies (Jacobs, Bowmaker, & Mollon, 1981). There is however substantial diversity in the relative positions of λ_{max} in the long- and short-wavelength cone pigments in mammals (Mollon, 1989; Nathans, 1987; Neitz & Jacobs, 1986). Thus, this mechanism, in its many manifestations in different species, can be regarded as the primordial basis for human color vision as it is common to all our mammalian ancestors (Mollon, 1989; Nathans, 1987), having emerged around 500 million years ago. Presumably, environmental factors such as the extent of nocturnal activity (and therefore ambient illumination), habitat, and feeding patterns strongly influenced the development of color vision in the early mammals (see Regan et al., 2001 for a review).

Of approximately 5000 mammals, only Old World monkeys, apes, and humans (i.e., catarrhines) plus New World Howler monkeys have developed uniform trichromatic color vision (Jacobs & Nathans, 2009; Jacobs, Neitz, Deegan, & Neitz, 1996). Fundamental questions in color science center on why and how this three dimensionality of color vision arose exclusively in these species. A particularly dominant (but not universally accepted) idea in this respect is that catarrhines came under strong evolutionary pressure to change their feeding behavior and, as a result, became frugivores (Mollon, 1989; Osorio & Vorobyev, 1996). It seems that these animals had already developed a substantial population of cones and post-receptoral neural circuitry, based on large numbers of small (midget) ganglion cells specialized to support high spatial resolution (Jacobs & Nathans, 2009; Regan et al., 2001; Wassle, 2004). As the chromaticities of many fruits occupy an extensive region in the middle- to long-wavelength regions of the visible spectrum, there was strong pressure to discriminate colored fruits against the green foliage of the trees or to identify tender, nutritionally rich fresh leaves whose color is slightly different from

their older counterparts (Lucas et al., 2003). Around 30–40 million years ago, foraging for fruit is thought to have favored the mutation of the long-wavelength cone, giving rise to two different cone types, one in the middle- and a second in the long-wavelength region of the visible spectrum (Mollon, 1989; Osorio & Vorobyev, 1996). It is therefore likely that this subsystem of color analysis was superimposed on a mechanism composed of a concentration of cone/midget ganglion cell connections that had developed primarily for high spatial resolution. One largely invariant environmental factor in the development of color processing in catarrhines is the role of sunlight, discussed above.

Color vision in the near peripheral visual field in humans

In the extreme periphery, human color vision is predominantly blue–yellow (Mullen & Kingdom, 2002; Murray, Parry, & McKeefry, 2006), reminiscent of that of lower mammals' color vision. However, at intermediate regions, around 10°–30°, a degree of trichromacy is maintained. Under controlled conditions, color vision remains largely unchanged within an eccentricity of around 10°. Beyond this, colors are described as "washed out" or reduced in saturation compared with central viewing. This loss of saturation is not uniform across all colors and eccentricities. At eccentricities of 20–25°, color stimuli that are signaled by the blue–yellow cone-opponent mechanism are remarkably unchanged in appearance (Parry et al., 2006), whereas those signaled by the red–green system exhibit substantial shifts in both their perceived hue and saturation (McKeefry, Murray, & Parry, 2007; Mullen, Sakurai, & Chu, 2005). These two attributes appear to vary independently of each other for a wide range of stimulus conditions (Parry et al., 2006), indicating they are underpinned by different neural mechanisms (McKeefry et al., 2007). It was suggested that if stimuli are large enough, color vision in the periphery becomes essentially the same as in the fovea (Abramov, Gordon, & Chan, 1991; Gordon & Abramov, 1977). However, as shown by Parry et al. (2006), this holds only for saturation, while hue shifts are evident regardless of the size of the stimulus. They also demonstrated that while most hues are distorted in the periphery, some remain remarkably unchanged for all eccentricities. Furthermore, those hues that remain stable with eccentricity (red, blue, yellow, and greenish blue) are independent of saturation (Panorgias, Kulikowski, Parry, McKeefry, & Murray, 2010) and stimulus size. Parry et al. referred to these as the peripherally invariant hues. Intriguingly, these particular colors do not correspond to the retina-based cardinal axes described above but rather are close to the four pure or non-reducible hues often referred to as the unique hues. Like peripherally invariant hues, the unique hues are largely independent of stimulus parameters, including eccentricity (Panorgias et al., 2010). Parry et al. (2006) found that invariant red, blue, and yellow match the unique hues identified in the peripheral field almost exactly for color normal observers.

In the present study, we set out to investigate how the phases of terrestrial illumination might have influenced stability and interobserver variation in peripheral color perception. Although our perception depends on reflected light from objects, the fact that illumination changes with such a conspicuous daily cycle is likely to have played some part in influencing the evolution of our color processing. We wanted to know how the modern and ancient roots of the two chromatic channels, along with the daylight phases, might determine the performance of two tests of color vision, color matching and color naming. These two techniques were used because it is thought that they reflect the operation of different mechanisms along the visual pathway. Color matching is determined by a retinal mechanism (Foster & Nascimento, 1994; Panorgias, Parry, McKeefry, Kulikowski, & Murray, 2009), while color naming depends mainly on cortical processing.

Methods

Observers

Thirty-eight (19 male and 19 female) observers (aged 26 ± 8 years, mean ± 1 *SD*) were recruited to the study. Most were university undergraduates. Color vision was tested with the Farnsworth-Munsell 100-Hue test, Ishihara plates (38-plate edition, 1979), and the Nagel anomaloscope Model 1. According to these tests, all had normal color vision. A further seven male observers were found to have a color vision defect and were therefore excluded from the study. All observers performed the asymmetric color-matching paradigm and 3 of them (an author (AP) and two others) also participated in a color-naming experiment. The three observers who conducted both experiments did so on separate days to avoid fatigue. The experiments followed the tenets of the Helsinki accord and ethical approval was obtained from the University of Manchester Ethics Committee.

Apparatus

Stimuli were presented on a CRT monitor (SONY Trinitron Multiscan520GS) controlled by a stimulus generator graphics card (ViSaGe, Cambridge Research Systems, Rochester, UK) driven by a PC. Prior to the

experiments, a calibration procedure was carried out, with a PR650 SpectraScan Colorimeter (Photo Research, Chatsworth, CA, U.S.A.) and a ColorCal (Cambridge Research Systems, Rochester, UK) to ensure that the stimulus chromaticities were presented accurately. Details of the calibration procedure can be found elsewhere (Parry et al., 2006).

The stimuli employed in this experiment were defined using CIE 1931 *xy* chromaticity coordinates. The rotation of a vector in CIE 1931 color space describes chromatic axis and its length describes purity. The 0°–180° and 90°–270° axes coincide with the cardinal L–M and S–(L + M) axes (Derrington, Krauskopf, & Lennie, 1984). A vector of length equal to 0.0739 was arbitrarily defined as purity of 1 and purity was linearly related to length. The monitor subtended 37.2° × 29.3° and the background chromaticity was equivalent to illuminant C (x = 0.31, y = 0.316) at 12.5 cd/m^2.

Matching experiment

A 1° diameter parafoveal spot was placed at 1° (nasal eccentricity) in order to avoid the peak macular pigment and the S-cone free zone (Williams, MacLeod, & Hayhoe, 1981). In addition, a 3° diameter peripheral spot (18° nasal eccentricity) was presented simultaneously for 380 ms (to avoid chromatic adaptation and involuntarily eye movements). Prior to the experiment, observers adapted to the background illuminant for ~10 min. The observer used a remote control (CB6, Cambridge Research Systems, Rochester, UK) to change the chromaticity of the peripheral spot to match that of the parafoveal stimulus. The two spots could be repeatedly presented to allow the observer to reach a satisfactory match. When this was achieved, the chromaticity of the parafoveal spot was changed, allowing the observer to determine the next match. In total, the parafoveal spot was presented at 24 chromaticities, from 0° to 360° in steps of 15° and always at 0.5 purity. After a 10-min break, the whole experiment was repeated.

Naming experiment

The procedure employed was a 4-alternative forced-choice (4AFC) naming paradigm (Parry et al., 2006). The observers were presented only with the peripheral 3° spot while they were fixating on a black cross. The spot was presented for 380 ms and the task was to name it as red, blue, green, or yellow. The chromaticities of the stimuli formed a circle in color space, as described above, but in this experiment the step was 9° instead of 15°. In total, 40 different chromaticities were used, all of saturation 0.5. Each color was presented randomly 20 times so that the observer named 800 stimuli in total. For each color category, a naming function was obtained. Each unique hue (i.e., red, blue, green, and yellow) was defined as the central maximum of the respective naming function.

Results

Figure 1 summarizes the results of both matching and naming experiments. The open circles, connected with a solid line, represent the averaged matches of the 38 observers. The dashed line depicts the Daylight Locus. The shaded area represents ±1 *SD* from the average curve. The four open diamonds show the average unique hues for the 3 observers who performed the naming task (see Table 1 for individual values).

The monitor background in Figure 1 is indicated by the point where the cardinal axes cross. The matching vector is the imaginary line linking this to each match point. The length of this vector varies with test chromaticity, indicating that there is greater perceived saturation loss across the 0°–180° cardinal (red–green) axis and that this is minimized for the blue and yellow–orange region. Unique blue and unique yellow are conspicuously close to the Daylight Locus, which intersects the probe circle at 120° and 283°.

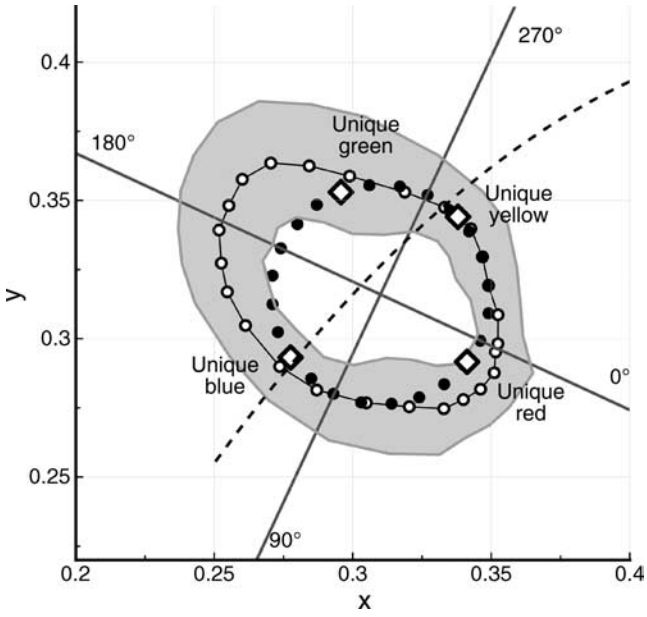

Figure 1. The average matches of 38 observers. The black dots are the probe chromaticities and the open circles are the corresponding matches. The gray shaded area depicts ±1 *SD* from the matches. The dashed curve is the Daylight Locus and the dark gray lines are the cardinal axes. Unique hues (open diamonds) are the average for three observers.

Observer	Unique red	Unique blue	Unique green	Unique yellow
HJT	12°	123°	228°	294°
AP	18°	121.5°	219°	288°
AD	9°	117°	225°	288°
Mean ± 1 *SD*	13° ± 4.6°	120° ± 3.1°	224° ± 4.6°	290° ± 3.5°

Table 1. Unique hues for 3 observers as defined by the naming paradigm at 18° eccentricity.

In Figure 2, hue (upper panel) and saturation (lower panel) are plotted separately. We tested several mathematical functions to describe these data and found 8th-order Fourier functions to provide the best fit. The dotted lines are the 95% confidence bounds of the fitted functions. The open diamonds are the unique hues and the dashed lines are the chromatic axes where the Daylight Locus intersects the circle describing probe chromaticities.

Hue rotation refers to the change in the chromatic axis of the test spot in order to match that of the probe. For example, Figure 2 shows that if the probe chromatic axis is 60°, the mean observer rotation of the test chromatic axis to obtain a match is approximately −20°. This means that he/she perceives the 40° hue as 60° while viewing it peripherally. The saturation graph shows the saturation of the test spot required to match that of the parafoveal spot. Thus, the saturation match for 60° is about 0.65, meaning that the average observer needed to increase purity of the test spot from 0.5 to 0.65.

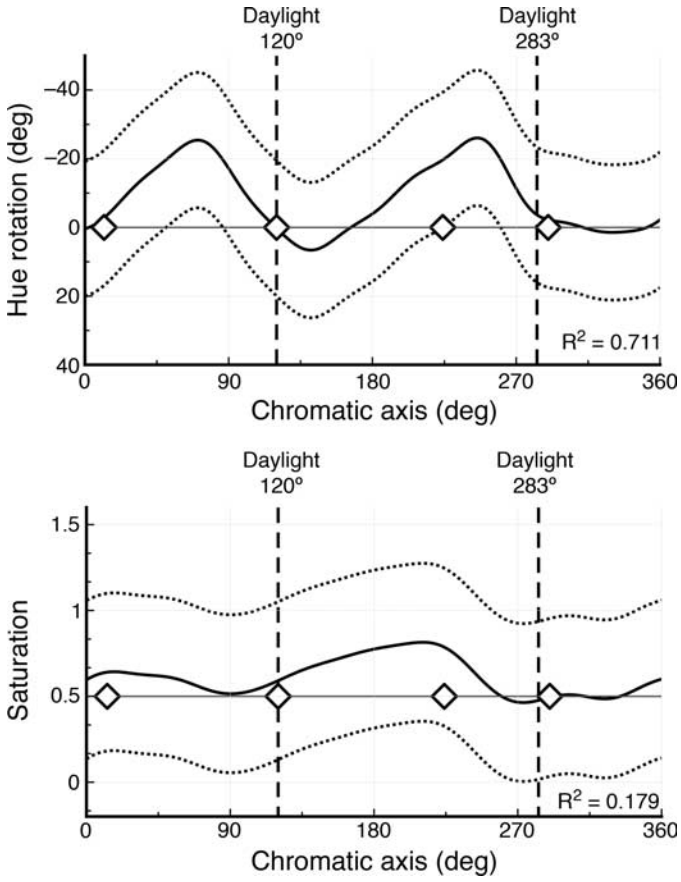

Figure 2. Hue rotation (upper panel) and saturation match (lower panel) for 38 observers. The black curves are fitted Fourier functions on the data. The dotted curves depict 95% confidence bounds. The dashed lines are the points where the Daylight Locus intersects the probe circle of 0.5 purity. The open diamonds are the averaged unique hues from 3 observers.

In the upper panel of Figure 2, it can be seen that there are two regions of major perceived hue shift at around 70° and 240° chromatic axes. At the point of unique blue and unique yellow, there is virtually no hue shift (0 on the vertical axis); the hues are perceived the same centrally and peripherally. In the lower panel, it is evident that there are areas where altering the saturation is required (in reddish and green-yellowish regions), while there are others where saturation is unchanged (around cardinal blue and the yellow-orangey region). It is clear that unique yellow coincides with an area where there is no need for saturation change, while unique blue corresponds to minimal saturation shift. It can be concluded that in the areas of color space close to unique blue and yellow color vision is more stable and less prone to changes that are the result of increasing retinal eccentricity. This is in contrast to color vision close to unique red and green that is subject to greater perceptual shifts with increasing retinal eccentricity.

Another common feature of unique blue and unique yellow is that both are almost coincident with the axes where the Daylight Locus intersects the probe circle, as has been reported previously (Mollon, 2006; Werner & Schefrin, 1993). Unique red is close to the minimum hue rotation point but needs increased saturation in the periphery (see Figures 1 and 2). Unique green is by no means close to either the minimum hue rotation point or the minimum saturation change. Thus, two interesting regions adjacent to the Daylight Locus can be identified, which exhibit the following characteristics: (1) their chromaticity shows no perceptual similarity to any other color (Wyszecki & Stiles, 1982) and (2) they show neither perceived hue shift nor saturation loss when retinal eccentricity is increased.

In order to determine how the intersubject variability changes around the color space and the extent to which it is influenced by the phases of daylight, a different approach to examining the data is employed. For each chromatic axis, there are 38 subjects per 2 trials = 76 data

points (matching points). For these 76 data points, ellipses are fitted using the least-squares criterion and an ellipse of the form:

$$ax^2 + bxy + cy^2 + dx + ey + f = 0. \quad (1)$$

The area of the fitted ellipse can then be regarded as an index of intersubject variability for that particular axis. The larger the area, the greater the variability is across observers for a particular axis, while a smaller area indicates less intersubject variability. Figure 3 shows five sets of data points for 0°, 90°, 120°, 210°, and 285° chromatic axes and the best-fitted ellipses around each data set.

From Figure 3, it can be seen that the elliptical area is smaller for the 285° and 90° axes, while it is larger for the 0° and 210° axes. Figure 4 plots the normalized elliptical area for all the chromatic axes (open circles).

The black curve is again a best-fitted 8th-order Fourier function. It can be seen that the area is minimized around the 105° and 290° chromatic axes and increases to reach maxima at 210° and 0° axes. Interestingly, it can be seen that from 0° up to ~105° the area, representing individual variability, gradually decreases. After 120°, there is a substantial increase in the area that remains stable up to 240°. Individual variability then rapidly decreases again as the 290° daylight point is approached reaching an obvious minimum that corresponds to unique yellow and the intersection with the Daylight Locus. In general, we can say that the intersubject variability is minimized around the Daylight Locus and that it is maximal in the red and green areas of color space. The interobserver variability is lowest for the yellow region.

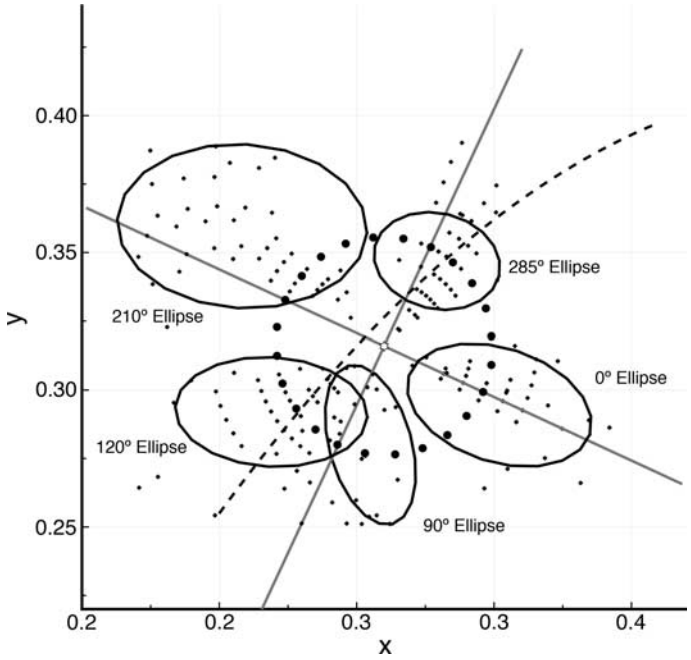

Figure 3. Fitted ellipses. The small dots show the raw matching data of 38 observers. Data shown here are for the 0°, 90°, 120°, 210°, and 285° axes. The ellipses are fitted using the least-squares method. The large dots are the probe chromaticities and the dashed curve is the Daylight Locus. The gray lines are the cardinal axes.

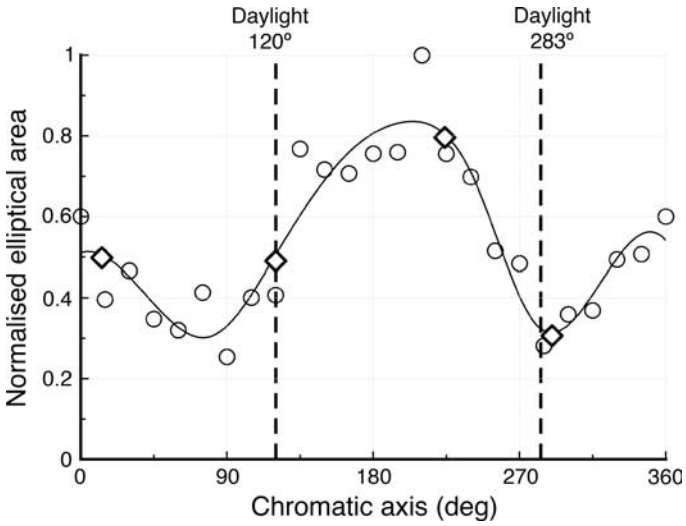

Figure 4. The elliptical area as a function of chromatic axis. The open circles depict the normalized elliptical area. The black curve is fitted on the data. The dashed lines are the Daylight Locus intersections with the probe circle. The open diamonds represent the four unique hues.

Discussion

The relatively large number of observers used in this study has enabled us to make three main observations. First, that intersubject variability in matching parafoveal and peripheral colored stimuli is markedly lower in regions of color space that correspond to the Daylight Locus. Second, peripherally invariant blue and yellow coincide with the Daylight Locus. Third, the blue and yellow unique hues, determined by a 4AFC-naming paradigm, also coincide with the Daylight Locus. These findings reinforce the notion that color vision of the higher primates and, in particular, those mechanisms that signal blue–yellow variation have been profoundly affected by the physical characteristics of daylight.

Peripherally invariant blue and yellow

As we have reported previously, across the visual field there are four hues that remain virtually unchanged as a function of eccentricity (McKeefry et al., 2007; Parry et al., 2006). Each of these corresponds to one of the red, blue, green, and yellow regions of color space, emphasizing

the idea that these colors represent anchor points for the organization of color information. It has been widely known for many years that in the far periphery our color vision becomes dichromatic (Moreland & Cruz, 1959). The superficial explanation for this phenomenon lies in the gross inhomogeneity in the distributions of cones: L- and M-cones are concentrated in clumps in the central retina (Roorda, Metha, Lennie, & Williams, 2001), whereas the more ancient S-cones are uniformly distributed outside the central 0.4° from which they are absent. The link between psychophysical tasks based on simple stimuli and retinal neurons has been extensively explored since Barlow (1972), but more contemporary views have also been presented (Lee, 2011). There is equally compelling evidence for the role of retinal physiology in color matching. For example, Panorgias et al. (2009) showed that there are quantitative differences in the nasal and temporal visual field for peripheral color matching and that these differences match the different distributions of cones and retinal ganglion cells either side of the midline in the retina. We would therefore assert that the matching task is predominantly subserved by retinal structures, although of course subsequent post-retinal structures affect the outcome of the experiments, as discussed below. Peripherally invariant blue and yellow, obtained using a matching technique, fall very close to the axes of the Daylight Locus. This is consistent with the interpretation that retinal mechanisms mediating this task have been strongly influenced by the phases of daylight.

Unique blue and yellow

In general, there is large interobserver variability in the settings of unique hues. We might ask to what extent our estimates of unique hues correspond to those in the literature. Webster, Miyahara, Malkoc, and Raker (2000) measured unique hues for 51 color normal observers and found that unique red is clustered around the cardinal red, the mean unique blue for these observers is at 477 ± 21 nm (mean ± 1 *SD*), unique green is at 541 ± 70 nm, and unique yellow is at 574 ± 10 nm. Unique red fell on the line of purples, where non-spectral colors are represented, and it was found to show least variation. Our unique hues can also be expressed in terms of dominant wavelengths. For the three observers who participated in the naming task, the mean unique blue is 482 ± 1 nm, unique green is 525 ± 7 nm, unique yellow is 578 ± 2 nm, and unique red is close to the cardinal red axis. These values are nearly identical to the values Schefrin and Werner (1990) obtained for 50 color normal observers. They found unique blue and yellow to be at 480 ± 6.4 nm and 577 ± 4.9 nm, respectively, for three luminance levels and across an age span from 13 to 74 years. Comparing these studies (but see also De Valois, De Valois, Switkes, & Mahon, 1997; Kuehni, 2004; Mollon, 2006; Wuerger, Atkinson, & Cropper, 2005), it can be concluded that the unique hues reported here are within the normal ranges of those described in the literature. Webster et al. (2000) reported mean unique blue, in terms of the chromatic axes employed in this study, being at 111° and unique yellow at 283°. It is evident that unique blue and yellow fall very close to the Daylight Locus (120° at the blue end and 283° at the yellow end) for the vast majority of observers.

One of the main reasons for identifying unique hues is that they reflect post-retinal activity and do not correspond with the retina-based cardinal axes. Instead, they represent exemplars of the four main phenomenological hue sensations: red, green, blue, and yellow. In the experiments reported here, it was felt important to tease apart cortical and retinal effects. There has been much discussion regarding the possibility of a cortical location for the coding of the unique hues (Abramov & Gordon, 2005; Wuerger et al., 2005). Mullen and Kulikowski (1990), in a 2 × 2AFC experiment, showed that wavelength discrimination at detection threshold occurs at a stage later than the photoreceptors and that the cone outputs are combined in different way than this in the cone-opponent process to give rise in the categorical boundaries of the spectrum. The primary visual cortex (Parkes, Marsman, Oxley, Goulermas, & Wuerger, 2009) and the posterior–inferior temporal cortex (Stoughton & Conway, 2008) have been considered as possible sites, but there are certain caveats to this idea (Conway & Stoughton, 2009; Mollon, 2009; Neitz & Neitz, 2008). It has been suggested that rather than having a specific neuronal basis, unique hues may arise from experience and be internalized by the mix of illuminants to which individuals are exposed in their everyday environment (Mollon, 2006). The peripheral hue-naming data presented here support the notion that the sensation of redness–greenness is mediated by cortical, or at least post-retinal, mechanisms that may or may not be "hard-wired" as discussed by Delahunt, Webster, Ma, and Werner (2004). From the perspective of our data, the blue–yellow mechanism is quite different. Unique blue and yellow and peripherally invariant blue and yellow correspond extremely well with the Daylight Locus and therefore imply dependence upon external illumination and some sort of normalization process as discussed by Delahunt et al. (2004).

The chromaticities of skylight and sunlight fall along a line that joins unique blue and unique yellow. This line, which Mollon (2006) described as the caerulean line (or the blue–yellow line), closely corresponds to the Daylight Locus (see Figure 5) for color temperatures between 4000 K and 25000 K (i.e., phases of daylight, as defined by the CIE; Wyszecki & Stiles, 1982, p. 6). Figure 5 plots the Daylight Locus, the caerulean line, and the unique hues measured in this report in the MacLeod–Boynton cone space. Notice that unique blue and unique yellow (measured in this case with non-spectral colors on a computer screen) are located almost exactly on the Daylight Locus (and the caerulean line) that describes the physical properties of these illuminants. This suggests

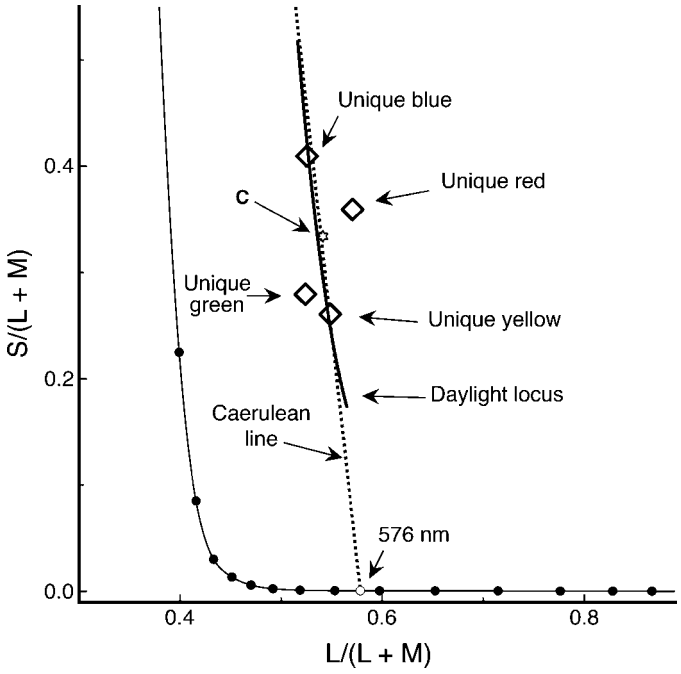

Figure 5. Unique hues plotted in the MacLeod–Boynton cone space. The thick line is the Daylight Locus between 4000 K and 25,000 K. The dotted line is the caerulean line (Mollon, 2006) connecting 576 nm (unique yellow) with 476 nm (unique blue). The open diamonds are the average unique hues from the three observers. The open star is illuminant C.

that the visual system is not affected by whether a light is multispectral, monochromatic, or if it is generated on a simulated environment such as a computer monitor or in physical space (Parry, Panorgias, McKeefry, & Murray, 2012). From the above, we can speculate that the two perceptual categorical hues, blue and yellow, have evolved under the influence of terrestrial illumination. Note, however, that this does not necessarily rule out some cortically located trigger features to account for that influence, as described above.

Interobserver variability

The ellipses described in Figure 3 represent population variability and should not be confused with MacAdam's (1942) ellipses or the works of Nagy, Eskew, and Boynton (1987) and Wyszecki and Fielder (1971) that are discrimination ellipses. The group of 38 observers shows a large interobserver variability in the green region and less variability in the red. Interestingly, the interobserver variability is minimal when the probe samples are relatively close to the Daylight Locus. Terrestrial illumination can be regarded as linked to this phenomenon for two reasons. First, L- and M-cones are highly polymorphic. Neitz and Jacobs (1990), Neitz, Neitz, and Jacobs (1993), and Neitz, Neitz, and Jacobs (1991) found that in an anomaloscope matching task color normal observers need different amounts of red and green to match a standard yellow. Analysis of the genotypes showed that an amino acid substitution in the photopigment opsin could produce a spectral shift of 5–7 nm in both L- and M-cones. This spectral variation is used to explain "a larger minimum color vision difference between individuals" as Neitz et al. (1993, p. 117) state and could explain the interobserver variability shown here. The chromatic cone-opponent L–M channel combines the signals of the two variable L- and M-cones, and the areas with maximum L–M cone-opponent activity are those where the larger interobserver variability is found. Intriguingly, the same highly variable L- and M-cones are combined to form the unique yellow, that is at 578 nm (or 285°), yet the interobserver variability is minimized at that point. The minimum interobserver variability in the unique yellow loci could be explained by the presence of a neural normalization routine that weights the L- and M-cone signals differently for each observer in order to obtain unique yellow. Perhaps, this has been tuned by this part of the Daylight Locus (Neitz, Carroll, Yamauchi, Neitz, & Williams, 2002). The same observation is proposed to explain the fact that, despite the highly variable L- to M-cone ratio in the color normal population from 0.6:1 to 12:1 (Carroll, McMahon, Neitz, & Neitz, 2000; Kremers et al., 2000), color perception, particularly of yellow, remains relatively constant. The color-matching ellipses presented here, as stated above, are attributed to the first and/or second stage of the visual pathway. This invites the proposition that it is not only higher order mechanisms that are normalized to give the perception of standard/unique yellow. Perhaps also the lower order mechanisms are subject to some form of normalization process.

A second line of reasoning is that there is better color discrimination along the Daylight Locus. Looking carefully at MacAdam's (1942) ellipses or at the more recent color-matching ellipses described by Wyszecki and Fielder (1971), it is evident that the elliptical area (which quantifies discrimination in that case) is highly variable, but it is reduced in the regions close to the Daylight Locus. Discrimination thresholds were measured around the categorical blue and yellow by Danilova and Mollon (2010), and they found that discrimination is again better along the Daylight Locus for non-saturated non-spectral colors. Note, however, that hue discrimination is not generally best at categorical "centroids" but at the categorical borders (Mullen & Kulikowski, 1990). This observation may not be very obvious when categories are narrow (blue and yellow) but becomes striking for the green category, whose centroid (at ~540 nm) is associated with poor wavelength discrimination. Conversely, at categorical borders with blue (~485 nm) and yellow (~555 nm), wavelength discrimination is best (see Figure 16.9 in Kulikowski & Walsh, 1991). The intersubject scatter seen in this paper (Figure 4) is a qualitatively similar function to the wavelength discrimination function,

although there is no explicit connection between them. However, they share the characteristic "W-shape" function (greatest scatter and poorer wavelength discrimination at the green category).

It is surely no coincidence that better discrimination, unique hues, invariant hues, and less variability in color-matching are observed in regions of color space occupied by the typical daily rhythm of terrestrial light. It is tempting to speculate that the relative stability of the blue–yellow system is due, at least in part, to natural illumination. The red–green system, on the other hand, is more variable both between and within observers and this might be due to the fact that variation along the red–green axis is dependent on reflected light from the plethora of objects in the visual environment that have a diverse range of reflectance spectra.

Acknowledgments

We would like to thank Jan Kremers for his constructive comments on an earlier version of the manuscript and all the reviewers for insightful remarks regarding wavelength discrimination. A. Panorgias received a stipend from the Visual Sciences Fund (Manchester). N. R. A. Parry is supported by the NIHR Manchester Biomedical Research Centre.

Commercial relationships: none.
Corresponding author: Athanasios Panorgias.
Email: apanorgias@ucdavis.edu.
Address: Vision Science and Retinal Imaging Laboratory, Department of Ophthalmology and Vision Science, University of California, Davis, 4860 Y Street, Suite 2400, Sacramento, CA 95817, USA.

References

Abramov, I., & Gordon, J. (2005). Seeing unique hues. *Journal of the Optical Society of America A, 22,* 2143–2153. [PubMed]

Abramov, I., Gordon, J., & Chan, H. (1991). Color appearance in the peripheral retina: Effects of stimulus size. *Journal of the Optical Society of America A, 8,* 404–414. [PubMed]

Barlow, H. B. (1972). Single units and sensation: A neuron doctrine for perceptual psychology? *Perception, 1,* 371–394. [PubMed]

Carroll, J., McMahon, C., Neitz, M., & Neitz, J. (2000). Flicker-photometric electroretinogram estimates of L:M cone photoreceptor ratio in men with photopigment spectra derived from genetics. *Journal of the Optical Society of America A, 17,* 499–509. [PubMed]

Conway, B. R., & Stoughton, C. M. (2009). Response: Towards a neural representation for unique hues. *Current Biology, 19,* 442–443.

Dacey, D. M. (2000). Parallel pathways for spectral coding in primate retina. *Annual Review of Neuroscience, 23,* 743–775. [PubMed]

Dacey, D. M., & Lee, B. B. (1994). The 'blue-on' opponent pathway in primate retina originates from a distinct bistratified ganglion cell type. *Nature, 367,* 731–735. [PubMed]

Danilova, M. V., & Mollon, J. D. (2010). Parafoveal color discrimination: A chromaticity locus of enhanced discrimination. *Journal of Vision, 10*(1):4, 1–9, http://www.journalofvision.org/content/10/1/4, doi:10.1167/10.1.4. [PubMed] [Article]

Delahunt, P. B., Webster, M. A., Ma, L., & Werner, J. S. (2004). Long-term renormalization of chromatic mechanisms following cataract surgery. *Visual Neuroscience, 21,* 301–307. [PubMed] [Article]

Derrington, A. M., Krauskopf, J., & Lennie, P. (1984). Chromatic mechanisms in lateral geniculate nucleus of macaque. *The Journal of Physiology, 357,* 241–265. [PubMed] [Article]

De Valois, R. L., De Valois, K. K., Switkes, E., & Mahon, L. (1997). Hue scaling of isoluminant and cone-specific lights. *Vision Research, 37,* 885–897. [PubMed]

Foster, D. H., & Nascimento, S. M. (1994). Relational color constancy from invariant cone-excitation ratios. *Proceedings of the Royal Society B, 257,* 115–121. [PubMed]

Gordon, J., & Abramov, I. (1977). Color vision in the peripheral retina: II. Hue and saturation. *Journal of the Optical Society of America, 67,* 202–207. [PubMed]

Hering, E. (1964). *Outlines of a theory of the light sense*. Cambridge, MA: Harvard University.

Hurvich, L. M., & Jameson, D. (1955). Some quantitative aspects of an opponent-colors theory: II. Brightness, saturation, and hue in normal and dichromatic vision. *Journal of the Optical Society of America, 45,* 602–616. [PubMed]

Jacobs, G. H. (2009). Evolution of color vision in mammals. *Philosophical Transactions of the Royal Society B, 364,* 2957–2967. [PubMed] [Article]

Jacobs, G. H., Bowmaker, J. K., & Mollon, J. D. (1981). Behavioural and microspectrophotometric measurements of color vision in monkeys. *Nature, 292,* 541–543. [PubMed]

Jacobs, G. H., & Deegan, J. F., 2nd. (1999). Uniformity of color vision in Old World monkeys. *Proceedings of the Royal Society B, 266,* 2023–2028. [PubMed] [Article]

Jacobs, G. H., & Nathans, J. (2009). The evolution of primate color vision. *Scientific American, 300,* 56–63. [PubMed]

Jacobs, G. H., Neitz, M., Deegan, J. F., & Neitz, J. (1996). Trichromatic color vision in New World monkeys. *Nature, 382,* 156–158. [PubMed]

Kremers, J., Scholl, H. P., Knau, H., Berendschot, T. T., Usui, T., & Sharpe, L. T. (2000). L/M cone ratios in human trichromats assessed by psychophysics, electroretinography, and retinal densitometry. *Journal of the Optical Society of America A, 17,* 517–526. [PubMed]

Kuehni, R. (2004). Variability in unique hue selection: A surprising phenomenon. *Color Research & Applications, 29,* 158–162.

Kulikowski, J. J., & Walsh, V. (1991). On the limits of color detection and discrimination. In J. J. Kulikowski, V. Walsh, & I. J. Murray (Eds.), *Limits of vision* (vol. 5, pp. 202–220). London: Macmillan Press.

Lee, B. B. (2011). Visual pathways and psychophysical channels in the primate. *The Journal of Physiology, 589,* 41–47. [PubMed] [Article]

Lucas, P. W., Dominy, N. J., Riba-Hernandez, P., Stoner, K. E., Yamashita, N., Loría-Calderón, E., Petersen-Pereira, W., Rojas-Durán, Y., Salas-Pena, R., Solis-Madrigal, S., Osorio, D., & Darvell, B. W. (2003). Evolution and function of routine trichromatic vision in primates. *Evolution, 57,* 2636–2643. [PubMed]

MacAdam, D. L. (1942). Visual sensitivities to color differences in daylight. *Journal of the Optical Society of America, 32,* 247–273.

McKeefry, D. J., Murray, I. J., & Parry, N. R. A. (2007). Perceived shifts in saturation and hue of chromatic stimuli in the near peripheral retina. *Journal of the Optical Society of America A, 24,* 3168–3179. [PubMed]

Mollon, J. D. (1989). "Tho' she kneel'd in that place where they grew…" The uses and origins of primate color vision. *Journal of Experimental Biology, 146,* 21–38. [PubMed]

Mollon, J. D. (2006). Monge: The Verriest lecture, Lyon, July 2005. *Visual Neuroscience, 23,* 297–309. [PubMed]

Mollon, J. D. (2009). A neural basis for unique hues? *Current Biology, 19,* R441–R442; author reply R442–R443. [PubMed]

Moreland, J. D., & Cruz, A. (1959). Color perception with the peripheral retina. *Optica Acta: International Journal of Optics, 6,* 117–151.

Mullen, K. T., & Kingdom, F. A. (2002). Differential distributions of red–green and blue–yellow cone opponency across the visual field. *Visual Neuroscience, 19,* 109–118. [PubMed]

Mullen, K. T., & Kulikowski, J. J. (1990). Wavelength discrimination at detection threshold. *Journal of the Optical Society of America A, 7,* 733–742. [PubMed]

Mullen, K. T., Sakurai, M., & Chu, W. (2005). Does L/M cone opponency disappear in human periphery? *Perception, 34,* 951–959. [PubMed]

Murray, I. J., Parry, N. R. A., & McKeefry, D. J. (2006). Cone opponency in the near peripheral retina. *Visual Neuroscience, 23,* 503–507. [PubMed]

Nagy, A. L., Eskew, R. T., Jr., & Boynton, R. M. (1987). Analysis of color-matching ellipses in a cone-excitation space. *Journal of the Optical Society of America A, 4,* 756–768. [PubMed]

Nathans, J. (1987). Molecular biology of visual pigments. *Annual Review of Neuroscience, 10,* 163–194. [PubMed]

Nayatani, Y., & Wyszecki, G. (1963). Color of daylight from north sky. *Journal of the Optical Society of America, 53,* 626–629.

Neitz, J., Carroll, J., Yamauchi, Y., Neitz, M., & Williams, D. R. (2002). Color perception is mediated by a plastic neural mechanism that is adjustable in adults. *Neuron, 35,* 783–792. [PubMed]

Neitz, J., & Jacobs, G. H. (1986). Polymorphism of the long-wavelength cone in normal human color vision. *Nature, 323,* 623–625. [PubMed]

Neitz, J., & Jacobs, G. H. (1990). Polymorphism in normal human color vision and its mechanisms. *Vision Research, 4,* 621–636. [PubMed]

Neitz, J., & Neitz, M. (2008). Color vision: The wonder of hue. *Current Biology, 18,* 700–702. [PubMed]

Neitz, J., Neitz, M., & Jacobs, G. H. (1993). More than three different cone pigments among people with normal color vision. *Vision Research, 33,* 117–122. [PubMed]

Neitz, M., Neitz, J., & Jacobs, G. H. (1991). Spectral tuning of pigments underlying red–green color vision. *Science, 252,* 971–974. [PubMed]

Osorio, D., & Vorobyev, M. (1996). Color vision as an adaptation to frugivory in primates. *Proceedings of the Royal Society B, 263,* 593–599. [PubMed]

Panorgias, A., Kulikowski, J. J., Parry, N. R. A., McKeefry, D. J., & Murray, I. J. (2010). Naming versus matching and the stability of unique hues. *Ophthalmic & Physiological Optics, 30,* 553–559. [PubMed]

Panorgias, A., Parry, N. R. A., McKeefry, D. J., Kulikowski, J. J., & Murray, I. J. (2009). Nasal–temporal differences in cone-opponency in the near peripheral retina. *Ophthalmic & Physiological Optics, 29,* 375–381. [PubMed]

Parkes, L. M., Marsman, J. B., Oxley, D. C., Goulermas, J. Y., & Wuerger, S. M. (2009). Multivoxel fMRI analysis of color tuning in human primary visual cortex. *Journal of Vision, 9*(1):1, 1–13, http://www.journalofvision.org/content/9/1/1, doi:10.1167/9.1.1. [PubMed] [Article]

Parry, N. R. A., McKeefry, D. J., & Murray, I. J. (2006). Variant and invariant color perception in the near peripheral retina. *Journal of the Optical Society of America A, 23,* 1586–1597. [PubMed]

Parry, N. R. A., Panorgias, A., McKeefry, D. J., & Murray, I. J. (2012). Real-world stimuli show perceived hue shifts in the peripheral visual field. *Journal of the Optical Society of America A, 29,* 96–101.

Regan, B. C., Julliot, C., Simmen, B., Vienot, F., Charles-Dominique, P., & Mollon, J. D. (2001). Fruits, foliage and the evolution of primate color vision. *Philosophical Transactions of the Royal Society of London B, 356,* 229–283. [PubMed] [Article]

Roorda, A., Metha, A. B., Lennie, P., & Williams, D. R. (2001). Packing arrangement of the three cone classes in primate retina. *Vision Research, 41,* 1291–1306. [PubMed]

Schefrin, B. E., & Werner, J. S. (1990). Loci of spectral unique hues throughout the life span. *Journal of the Optical Society of America A, 7,* 305–311. [PubMed]

Shepard, R. N. (1992). The perceptual organization of colors: An adaptation to regularities of the terrestrial world. In J. H. Barkow, L. Cosmides, & J. Tooby (Eds.), *The adapted mind* (pp. 495–532). New York: Oxford University Press.

Smith, G. S. (2005). Human color vision and the unsaturated blue color of the daytime sky. *American Journal of Physics, 73,* 590–597.

Stoughton, C. M., & Conway, B. R. (2008). Neural basis for unique hues. *Current Biology, 18,* 698–699. [PubMed]

Wassle, H. (2004). Parallel processing in the mammalian retina. *Nature Reviews Neuroscience, 5,* 747–757. [PubMed]

Webster, M. A., Miyahara, E., Malkoc, G., & Raker, V. E. (2000). Variations in normal color vision: II. Unique hues. *Journal of the Optical Society of America A, 17,* 1545–1555. [PubMed]

Werner, J. S., & Schefrin, B. E. (1993). Loci of achromatic points throughout the life span. *Journal of the Optical Society of America A, 10,* 1509–1516. [PubMed]

Williams, D. R., MacLeod, D. I., & Hayhoe, M. M. (1981). Foveal tritanopia. *Vision Research, 21,* 1341–1356. [PubMed]

Wuerger, S. M., Atkinson, P., & Cropper, S. (2005). The cone inputs to the unique-hue mechanisms. *Vision Research, 45,* 3210–3223. [PubMed]

Wyszecki, G., & Fielder, G. H. (1971). New color-matching ellipses. *Journal of the Optical Society of America, 61,* 1135–1152. [PubMed]

Wyszecki, G., & Stiles, W. S. (1982). *Color science; concepts, methods and quantitative data and formulae* (2nd ed.). New York: Wiley.